ChemComm

COMMUNICATION

View Article Online
View Journal | View Issue

Open Access Article. Published on 22 June 2021. Downloaded on 3/25/2026 10:19:36 AM.
This article is licensed under a Creative Commons Attribution 3.0 Unported Licence.

Check for updates

Cite this: *Chem. Commun.*, 2021, **57**, 7132

Received 2nd June 2021,
Accepted 22nd June 2021

DOI: 10.1039/d1cc02912f

rsc.li/chemcomm

Cluster expansion and vertex substitution pathways in nickel germanide Zintl clusters†

Oliver P. E. Townrow,[a] Andrew S. Weller *[b] and Jose M. Goicoechea *[a]

We describe the reactivity of the hypersilyl-functionalized Zintl cluster salt K[$Ge_9(Hyp)_3$] towards the nickel reagents $Ni(COD)_2$ and $Ni(Cp)_2$, which gives rise to markedly different complexes. In the case of $Ni(COD)_2$ (COD = 1,5-cyclooctadiene), a dianionic sandwich-like cluster $[Ni\{Ge_9(Hyp)_3\}_2]^{2-}$ (1) was obtained, in line with a simple ligand substitution reaction of COD by $[Ge_9(Hyp)_3]^-$. By contrast, when an analogous reaction with $Ni(Cp)_2$ (Cp = cyclopentadienyl) was performed, vertex substitution of the $[Ge_9(Hyp)_3]^-$ precursor was observed, giving rise to the nine-vertex *nido*-cluster (Cp)Ni[$Ge_8(Hyp)_3$] (2). This is the first instance of vertex substitution at a hypersilyl-functionalized Zintl cluster cage. The electrochemical behavior of these compounds was explored and showed reversible redox behaviour for both clusters.

Intermetallic materials consisting of nickel and germanium (nickel germanides) have been recently explored as catalysts,[1] components in microelectronics,[2] and thermoelectric materials.[3] Methods for the preparation of such compounds include atomic layer deposition and direct current (DC) or radio frequency (RF) sputtering, which allow for the preparation of high purity samples. Given the important technological applications of such materials, the development of alternative synthetic techniques based on well-defined molecular precursors is an attractive prospect. In this context, one such family of compounds that are of interest are heteroatomic Zintl clusters composed of main group and transition metal elements.[4] These soluble molecular species can be viewed as mimics of binary intermetallic compounds.[5] As far as nickel germanide clusters are concerned, an array of species with varying compositions have been isolated to date such as $[Ni@Ge_9]^{3-}$,[6] $[Ni@Ge_9Ni(CO)]^{3-}$,[6] $[Ni_3@(Ge_9)_2]^{4-}$,[7] and $[Ge_5Ni_2(CO)_3]^{2-}$.[8] The formation of many of such clusters, $[Ni_2@Ge_{14}Ni_4(CO)_5]^{4-}$ for example,[9] involves cluster-fragmentation pathways that are poorly understood owing to the lack of suitable spectroscopic handles to monitor such reactions. This aspect of Zintl cluster chemistry – the mechanisms by which an otherwise robust molecular precursor, such as the nonagermanide tetra-anion, $[Ge_9]^{4-}$, redistributes in solution to afford higher nuclearity clusters – remains for the most part a mystery, although recently some studies have aimed to elucidate viable pathways.[10]

In an effort to probe such reactivity, we have recently become interested in studying the tris-functionalised nonagermanide cluster $[Ge_9(Hyp)_3]^-$ (Hyp = $Si(SiMe_3)_3$).[11] Over the last ten years this species has received significant attention as a supporting ligand for transition metals.[12–15] For example, we recently reported its use in the synthesis of a novel Rh-based homogeneous catalyst for the hydrogenation of cyclic alkenes.[15] The principal advantages of $[Ge_9(Hyp)_3]^-$ as a ligand are that it is (highly) soluble in non-polar aprotic solvents, and that reactions can be studied in greater detail using solution NMR spectroscopic techniques given the presence of ^1H and ^{29}Si nuclei in the hypersilyl substituents. A number of metal-containing clusters have been isolated containing this cluster as a support, that exhibit a variety of coordination modes (η^1, η^3, η^4, η^5), which depend on the electronic requirement of the metal centres in question.[12–15] Empirical observations also suggest that the $[Ge_9(Hyp)_3]^-$ precursor is less prone to fragmentation than that of its unsubstituted counterpart $[Ge_9]^{4-}$.[4,16]

In addition to *cluster expansion* reactions, whereby higher nuclearity clusters form on reaction of Zintl clusters with transition metal reagents, another interesting class of reactions are those in which a transition metal fragment replaces one of the cluster vertices, so-called *vertex substitution* reactions.[17] It has been postulated that vertex substitution of $[E_9]^{4-}$ clusters (E = Ge, Sn, Pb) may be an early step towards cluster expansion, whereby the fragmented cluster combines with another to form higher nuclearity cages.[10,18] Some examples of clusters which have undergone vertex substitution reactions include

[a] *Department of Chemistry, University of Oxford, Chemistry Research Laboratory, 12 Mansfield Road, Oxford, OX1 3TA, UK. E-mail: jose.goicoechea@chem.ox.ac.uk*
[b] *Department of Chemistry, University of York, YO10 5DD, UK. E-mail: andrew.weller@york.ac.uk*

† Electronic supplementary information (ESI) available: Experimental details, analytical data, spectra and computational methods. CCDC 2087498 and 2087499. For ESI and crystallographic data in CIF or other electronic format see DOI: 10.1039/d1cc02912f

This journal is © The Royal Society of Chemistry 2021

Open Access Article. Published on 22 June 2021. Downloaded on 3/25/2026 10:19:36 AM.
This article is licensed under a Creative Commons Attribution 3.0 Unported Licence.

$[(Cp)TiSn_8]^{3-}$ and $[(CO)_3FeGe_8]^{3-}$,[18,19] both of which exhibit cluster topologies encountered in higher nuclearity clusters such as $[Ni_2@Sn_{17}]^{4-}$.[20] The mechanisms involved in these processes remain poorly understood, largely because of the lack of methods to study the solution behaviour. Establishing complementary reactivity in their functionalized, more soluble counterparts may allow us to monitor these processes.

Herein, we report the reactions of homoleptic nickel organometallics $Ni(COD)_2$ (COD = 1,5-cyclooctadiene) and $Ni(Cp)_2$ (Cp = cyclopentadienyl), both well studied precursors and dopants for Ni containing materials,[21,22] with $K[Ge_9(Hyp)_3]$. These studies show that the nature of the nickel precursor has a significant effect on the clusters formed in solution. Using $Ni(COD)_2$ results in cluster expansion, while in contrast $Ni(Cp)_2$ replaces one of the germanium vertices of the $[Ge_9(Hyp)_3]^-$ cluster, in a vertex substitution reaction.

The reaction of $Ni(COD)_2$ and two equivalents of $K[Ge_9(Hyp)_3]$ in benzene or toluene results in the formation of a dark green solution, presumably of the complex $K_2[Ni\{Ge_9(Hyp)_3\}_2]$ (K_2[**1**]).‡ This product is unstable in solution for more than 2 days and also if placed under vacuum, forming a brown suspension from which the previously reported $[K(tol)_3][Ge_9(Hyp)_3]\cdot$tol was recovered from toluene.[23] However, addition of 2,2,2-crypt (4,7,13,16,21,24-hexaoxa-1,10-diazabicyclo[8.8.8]-hexacosane) to the reaction mixture allows for the isolation of the dianionic formally Ni(0) sandwich compound $[K(2,2,2\text{-crypt})]_2[Ni\{Ge_9(Hyp)_3\}_2]$ ($[K(2,2,2\text{-crypt})]_2$[**1**]), which is sparingly soluble in THF (Scheme 1).

Dark green-blue crystals suitable for single crystal X-ray crystallography were grown from a concentrated THF solution at −40 °C. The cluster adopts a D_{3d} symmetric sandwich-like geometry in which the central Ni atom is coordinated by a triangular face of each of the two flanking clusters (Fig. 1). The coordinated Ge–Ge distances are elongated by ∼0.2 Å compared with the non-coordinated face of the cluster. The dianionic cluster **1** is valence isoelectronic with related clusters such $[M[Ge_9(Hyp)_3]_2]$ (M = Zn–Hg) and $[Au[Ge_9(Hyp)_3]_2]^-$.[13i,j] There is also a close structural relationship to the substituent-free species $[Ni_3@(Ge_9)_2]^{4-}$,[7] although it is notable that the Ni–Ge bond lengths in **1** are *ca.* 0.1 Å shorter, 2.436(1)–2.443(1) Å, (*cf.* 2.505(1)–2.540(1) Å in $[Ni_3@(Ge_9)_2]^{4-}$), which is presumably due to the absence of interstitial nickel atoms in the former, and its reduced overall charge.

NMR spectroscopic analysis of **1** shows one hypersilyl singlet resonance in the ^{1}H NMR spectrum at 0.38 ppm as well as resonances at 2.58, 3.57 and 3.61 ppm from the two $[K(2,2,2\text{-crypt})]^+$ counter-ions. $^{13}C\{^1H\}$ and $^1H/^{29}Si$ HMBC NMR spectra are in agreement with retention of the D_{3d} geometry in solution, the latter exhibiting two ^{29}Si NMR resonances with two cross-peaks. This is as expected from the symmetry observed in the solid state. Owing to decomposition *via* fragmentation in solution, a small amount (∼3%) of the previously reported $[K(2,2,2\text{-crypt})][Ge_9(Hyp)_3]$ is also present (see ESI†).

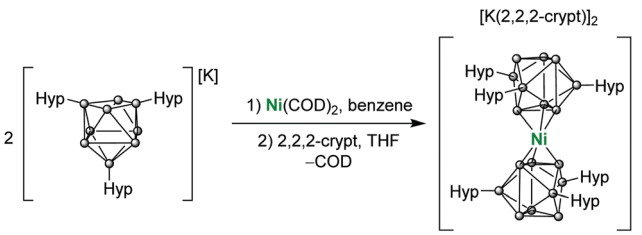

Scheme 1 Preparation of $[K(2,2,2\text{-crypt})]_2[Ni\{Ge_9(Hyp)_3\}_2]$ ($[K(2,2,2\text{-crypt})]_2$[**1**]).

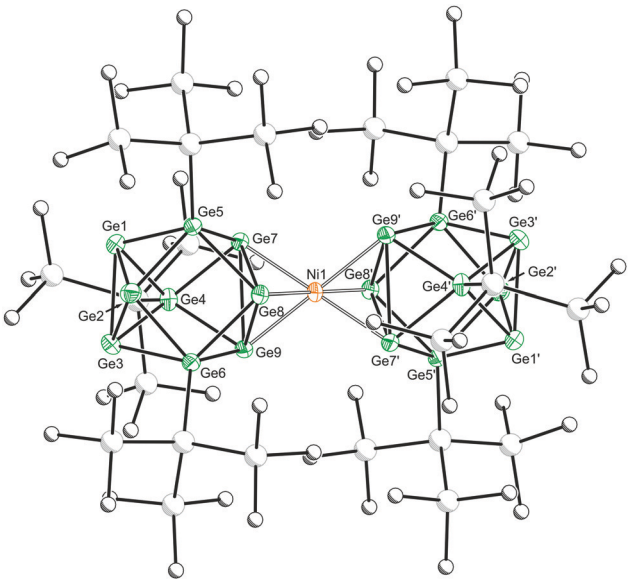

Fig. 1 Molecular structure of $[K(2,2,2\text{-crypt})]_2$[**1**]·2THF. Anisotropic displacement ellipsoids are set at 50% probability. Hydrogen atoms, $[K(2,2,2\text{-crypt})]^+$, and solvent of crystallisation have been omitted for clarity. Carbon and silicon atoms are pictured as spheres of arbitrary radii. Selected bond distances [Å]: Ni1–Ge7:2.442(1), Ni1–Ge8:2.436(1), Ni1–Ge9:2.443(1), Ge1–Ge2:2.679(1), Ge1–Ge3:2.643(1), Ge2–Ge3:2.631(1), Ge7–Ge8:2.900(1), Ge7–Ge9:2.830(1), Ge8–Ge9:2.826(1). Symmetry operation ′: 1 − *x*, 1 − *y*, −*z*.

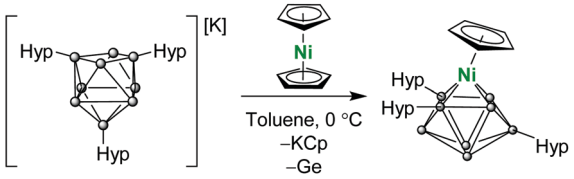

Scheme 2 Preparation of $(Cp)Ni[Ge_8(Hyp)_3]$ (**2**).

In an attempt to isolate a mixed sandwich complex, we turned our attention to the reaction of $Ni(Cp)_2$ or $(Cp)Ni(PPh_3)Cl$ with $K[Ge_9(Hyp)_3]$, however both reactions resulted in vertex substitution, whereby a germanium atom of the cluster cage is replaced by a (Cp)Ni fragment, producing the neutral cluster $(Cp)Ni[Ge_8(Hyp)_3]$ (**2**; Scheme 2). Vertex substitution has been previously observed for unsubstituted $[E_9]^{4-}$ (E = Ge, Sn) clusters,[17–19] performed in highly polar solvents under reducing conditions, however such transformations are unprecedented for functionalized precursors such as $[Ge_9(Hyp)_3]^-$.

Emerald green crystals of **2** suitable for single crystal X-ray crystallography were grown from a concentrated solution of toluene (Fig. 2). The cluster adopts a C_s-symmetric distorted

Open Access Article. Published on 22 June 2021. Downloaded on 3/25/2026 10:19:36 AM.
This article is licensed under a Creative Commons Attribution 3.0 Unported Licence.

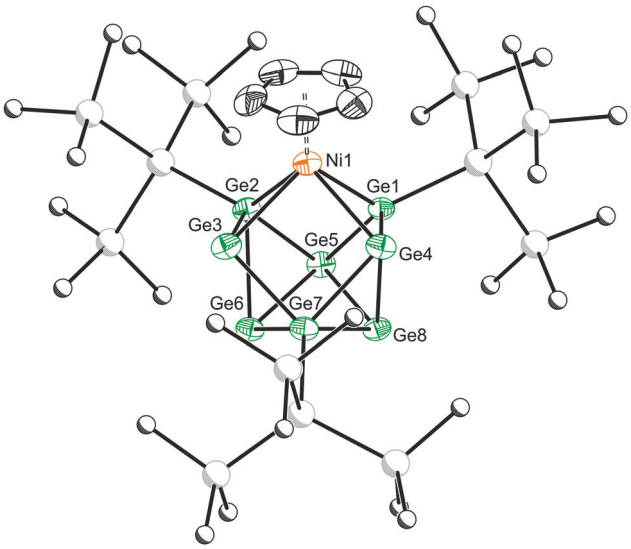

Fig. 2 Molecular structure of **2**·1.5tol. Anisotropic displacement ellipsoids are set at 50% probability. Hydrogen atoms and solvent of crystallisation have been omitted for clarity. Carbon and silicon atoms are pictured as spheres of arbitrary radii. Selected bond distances [Å]: Ni1–Ge1:2.400(2); Ni1–Ge2:2.404(2); Ni1–Ge3:2.591(2); Ni1–Ge4:2.580(2).

mono-capped square-antiprismatic geometry, with the Ni(Cp) moiety occupying a basal position. This cluster can be described as a *nido*-deltahedron with 22 electrons available for cluster bonding.[24] Structurally, this cluster is closely related to $[(Cp)TiSn_8]^{3-}$ and $[(CO)_3FeGe_8]^{3-}$.[18,19]

The NMR spectroscopic data are in agreement with the solid state structure, exhibiting two ^{1}H NMR resonances for the hypersilyl environments at 0.49 and 0.60 ppm in a 2 : 1 ratio, in addition to a single resonance for the C_5H_5 ligand at 5.18 ppm. In addition to this, $^{13}C\{^1H\}$ and $^1H/^{29}Si$ HMBC NMR supply further evidence for the two inequivalent hypersilyl environments, with four cross peaks observed in the HMBC spectrum.

The structural relationship and contrasting electron counts between **2** and $[(CO)_3FeGe_8]^{3-}$ (22 and 21 clusters bonding electrons, respectively), point to the possibility of facile redox processes. We were intrigued to explore the electrochemical behaviour of these clusters through a series of cyclic voltammetry (CV) studies.

The dianionic sandwich complex **1** features a reversible oxidation at $E_1^0 = -1.56$ V (Fig. 3), which is followed by a second, quasi-reversible oxidation event at $E_2^0 = -1.20$ V (all potentials given relative to the ferrocene/ferrocenium redox couple; $Fc^{0/+} = 0$). This is followed by a third oxidation ($E_3^{pa} = -0.85$ V *vs.* $Fc^{0/+}$) which is irreversible at all scan rates ($\nu = 0.05$–1 mV s^{-1}). To date, this is only the second observation of reversible redox behaviour for solutions of Zintl clusters.[25] However, attempts to chemically access these oxidized clusters by, for example, oxidation with cobaltocenium hexafluorophosphate were unsuccessful. This leads us to believe that while oxidized clusters may be kinetically accessible, they cannot be accessed because of decomposition.

Electrochemical analysis of **2** features a reversible reductive event at $E_1^0 = -2.07$ V. This is followed by a second reduction at $E_2^{pc} = -2.54$ V, which is irreversible at all scan

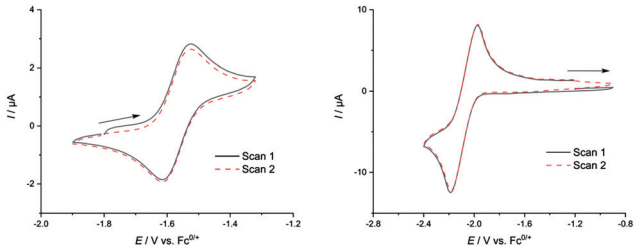

Fig. 3 Cyclic voltammogram of complexes **1** (left; 100 mV s^{-1}; first oxidative event; 1.0 mM, 0.2 M $[NBu_4][PF_6]$, THF, room temperature) and **2** (right; 100 mV s^{-1}; first reductive event; 1.0 mM, 0.1 M $[NBu_4][PF_6]$, THF, room temperature). Arrows indicated starting points of scans and their direction.

rates ($\nu = 0.05$–1 mV s^{-1}) and is accompanied by two additional irreversible features in the reverse scan ($E^{pa} = -2.38$, -1.21 V) indicating some form of cluster degradation/rearrangement on over-reduction. Attempts to access this compound *via* reduction with a Na/Hg amalgam gave rise to a complex ^{1}H NMR spectrum, indicative of excessive cluster decomposition. As with **1**, it would appear that while these reversible reductive redox events are observable in the cyclic voltammetry measurements, chemical isolation of these compounds is challenging. Interestingly, and despite the precedent for a closely related oxidized cluster, $[(CO)_3Fe(Ge_8)]^{3-}$, no oxidation events were observed in the CV scans.

We have shown that two distinct reactivity pathways are accessible for the functionalised Zintl cluster $[Ge_9(Hyp)_3]^-$ on reaction with nickel reagents. In the case of the nickel(0) precursor $Ni(COD)_2$ simple ligand displacement gives rise to the sandwich type compound $[Ni\{Ge_9(Hyp)_3\}_2]^{2-}$, and cluster expansion. By contrast, reactions with the nickel(II) reagents $Ni(Cp)_2$ or $(Cp)Ni(PPh_3)Cl$ were found to give rise to vertex-substitution reactions, whereby a germanium atom of the $[Ge_9(Hyp)_3]^-$ cluster is replaced by a Ni(Cp) moiety. This is the first example of such a transformation involving functionalized Zintl clusters such as $[Ge_9(Hyp)_3]^-$. While the reaction mechanism for such a transformation remains unknown, the high yield in which this compound can be obtained should allow for further reactivity studies.

We thank Shell Global Solutions International B. V., the EPSRC and the University of Oxford for financial support of this research (Industrial CASE studentship O. P. E. T.). The University of Oxford is also acknowledged for access to Chemical Crystallography facilities.

Conflicts of interest

There are no conflicts to declare.

Notes and references

‡ See ESI for all experimental details.

1 (*a*) J. Y. Chen, S. L. Jheng and H. Y. Tuan, *Nanoscale*, 2018, **10**, 11072–11078; (*b*) P. W. Menezes, S. Yao, R. Beltrán-Suito, J. N. Hausmann, P. V. Menezes and M. Driess, *Angew. Chem., Int. Ed.*, 2021, **60**, 4640–4647.

 This journal is © The Royal Society of Chemistry 2021

Open Access Article. Published on 22 June 2021. Downloaded on 3/25/2026 10:19:36 AM.
This article is licensed under a Creative Commons Attribution 3.0 Unported Licence.

2 (*a*) B. De Schutter, K. Van Stiphout, N. M. Santos, E. Bladt, J. Jordan-Sweet, S. Bals, C. Lavoie, C. M. Comrie, A. Vantomme and C. Detavernier, *J. Appl. Phys.*, 2016, **119**, 135305; (*b*) T. Grzela, G. Capellini, W. Koczorowski, M. A. Schubert, R. Czajka, N. J. Curson, I. Heidmann, T. Schmidt, J. Falta and T. Schroeder, *Nanotechnology*, 2015, **26**, 385701; (*c*) M. Sheehan, Y. Guo, G. Flynn, H. Geaney and K. M. Ryan, *CrystEngComm*, 2017, **19**, 2072–2078; (*d*) M. Swain, S. Singh, D. Bhattacharya, A. Singh, R. B. Tokas, C. L. Prajapat and S. Basu, *AIP Adv.*, 2015, **5**, 077129; (*e*) C. Yan, J. M. Higgins, M. S. Faber, P. S. Lee and S. Jin, *ACS Nano*, 2011, **5**, 5006–5014; (*f*) S. Zhu and A. Nakajima, *Jpn. J. Appl. Phys., Part 2*, 2005, **44**, L753.
3 (*a*) K. Kim, S. Mun, M. Jang, J. Sok and K. Park, *Appl. Phys. A: Mater. Sci. Process.*, 2021, **127**, 50; (*b*) M. Noroozi, B. Hamawandi, M. S. Toprak and H. H. Radamson, *ULIS 2014–2014 15th*Int. Conf. Ultim. Integr. Silicon, IEEE Computer Society, 2014, 125–128.
4 For review articles see: (*a*) B. Weinert, S. Mitzinger and S. Dehnen, *Chem. – Eur. J.*, 2018, **24**, 8470–8490; (*b*) R. J. Wilson, B. Weinert and S. Dehnen, *Dalton Trans.*, 2018, **47**, 14861–14869; (*c*) B. Weinert and S. Dehnen, *Struct. Bonding*, 2017, **174**, 99–134; (*d*) N. Korber, *Angew. Chem., Int. Ed.*, 2009, **48**, 3216–3217; (*e*) S. C. Sevov and J. M. Goicoechea, *Organometallics*, 2006, **25**, 5678–5692.
5 For a recent review of intermetalloid clusters see: K. Mayer, J. Weßing, T. F. Fässler and R. A. Fischer, *Angew. Chem., Int. Ed.*, 2018, **57**, 14372–14393.
6 J. M. Goicoechea and S. C. Sevov, *J. Am. Chem. Soc.*, 2006, **128**, 4155–4161.
7 J. M. Goicoechea and S. C. Sevov, *Angew. Chem., Int. Ed.*, 2005, **117**, 4094–4096.
8 C. Liu, L. J. Li, Q. J. Pan and Z. M. Sun, *Chem. Commun.*, 2017, **53**, 6315–6318.
9 E. N. Esenturk, J. Fettinger and B. Eichhorn, *Polyhedron*, 2006, **25**, 521–529.
10 (*a*) C. Zhang, H. W. T. Morgan, Z. C. Wang, C. Liu, Z. M. Sun and J. E. McGrady, *Dalton Trans.*, 2019, **48**, 15888–15895; (*b*) S. Mitzinger, L. Broeckaert, W. Massa, F. Weigend and S. Dehnen, *Nat. Commun.*, 2016, **7**, 1–10; (*c*) J. Q. Wang, S. Stegmaier, B. Wahl and T. F. Fässler, *Chem. – Eur. J.*, 2010, **16**, 1793–1798.
11 (*a*) F. Li and S. C. Sevov, *Inorg. Chem.*, 2012, **51**, 2706–2708; (*b*) A. Schnepf, *Angew. Chem., Int. Ed.*, 2003, **42**, 2624–2625.
12 For examples of η^1-$[Ge_9R_3]^-$ clusters see: (*a*) F. S. Geitner, W. Klein, O. Storcheva, T. D. Tilley and T. F. Fässler, *Inorg. Chem.*, 2019, **58**, 13293–13298; (*b*) N. C. Michenfelder, C. Gienger, A. Schnepf and A. N. Unterreiner, *Dalton Trans.*, 2019, **48**, 15577–15582.
13 For examples of η^3-$[Ge_9R_3]^-$ clusters see: (*a*) L. J. Schiegerl, M. Melaimi, D. R. Tolentino, W. Klein, G. Bertrand and T. F. Fässler, *Inorg. Chem.*, 2019, **58**, 3256–3264; (*b*) O. Kysliak, D. D. Nguyen, A. Z. Clayborne and A. Schnepf, *Inorg. Chem.*, 2018, **57**, 12603–12609; (*c*) F. S. Geitner, M. A. Giebel, A. Pöthig and T. F. Fässler, *Molecules*, 2017, **22**, 1204; (*d*) F. S. Geitner and T. F. Fässler, *Eur. J. Inorg. Chem.*, 2016, 2688–2691; (*e*) O. Kysliak, C. Schrenk and A. Schnepf, *Chem. – Eur. J.*, 2016, **22**, 18787–18793; (*f*) K. Mayer, L. J. Schiegerl and T. F. Fässler, *Chem. – Eur. J.*, 2016, **22**, 18794–18800; (*g*) F. Li and S. C. Sevov, *Inorg. Chem.*, 2015, **54**, 8121–8125; (*h*) C. Schenk, F. Henke, G. Santiso-Quiñones, I. Krossing and A. Schnepf, *Dalton Trans.*, 2008, 4436–4441; (*i*) F. Henke, C. Schenk and A. Schnepf, *Dalton Trans.*, 2009, 9141–9145; (*j*) C. Schenk and A. Schnepf, *Angew. Chem., Int. Ed.*, 2007, **46**, 5314–5316.
14 For examples of η^5-$[Ge_9R_3]^-$ clusters see: (*a*) S. Frischhut, F. Kaiser, W. Klein, M. Drees, F. E. Kühn and T. F. Fässler, *Organometallics*, 2018, **37**, 4560–4567; (*b*) F. Li, A. Muñoz-Castro and S. C. Sevov, *Angew. Chem., Int. Ed.*, 2016, **55**, 8630–8633; (*c*) F. Henke, C. Schenk and A. Schnepf, *Dalton Trans.*, 2011, **40**, 6704–6710; (*d*) C. Schenk and A. Schnepf, *Chem. Commun.*, 2009, 3208–3210.
15 O. P. E. Townrow, C. Chung, S. A. Macgregor, A. S. Weller and J. M. Goicoechea, *J. Am. Chem. Soc.*, 2020, **142**, 18330–18335.
16 D. R. Gardner, J. C. Fettinger and B. W. Eichhorn, *Angew. Chem., Int. Ed. Engl.*, 1996, **35**, 2852–2854.
17 For a recent example of vertex substitution reactions in Zintl cluster chemistry see: A. M. Li, Y. Wang, P. Y. Zavalij, F. Chen, A. Muñoz-Castro and B. W. Eichhorn, *Chem. Commun.*, 2020, **56**, 10859–10862.
18 C. B. Benda, M. Waibel and T. F. Fässler, *Angew. Chem., Int. Ed.*, 2015, **54**, 522–526.
19 B. Zhou and J. M. Goicoechea, *Chem. – Eur. J.*, 2010, **16**, 11145–11150.
20 E. N. Esenturk, A. J. C. Fettinger and B. W. Eichhorn, *J. Am. Chem. Soc.*, 2006, **128**, 12–13.
21 (*a*) J. Bachmann, A. Zolotaryov, O. Albrecht, S. Goetze, A. Berger, D. Hesse, D. Novikov and K. Nielsch, *Chem. Vap. Deposition*, 2011, **17**, 177–180; (*b*) S.-D. Hwang, *J. Vac. Sci. Technol., B: Microelectron. Nanometer Struct. –Process., Meas., Phenom.*, 1996, **14**, 2957; (*c*) M. V. Kharlamova, M. Sauer, T. Saito, Y. Sato, K. Suenaga, T. Pichler and H. Shiozawa, *Nanoscale*, 2015, **7**, 1383–1391; (*d*) J. A. Singh, N. F. W. Thissen, W. H. Kim, H. Johnson, W. M. M. Kessels, A. A. Bol, S. F. Bent and A. J. M. MacKus, *Chem. Mater.*, 2018, **30**, 663–670.
22 (*a*) J. S. Bradley, B. Tesche, W. Busser, M. Maase and M. T. Reetz, *J. Am. Chem. Soc.*, 2000, **122**, 4631–4636; (*b*) N. J. S. Costa, R. F. Jardim, S. H. Masunaga, D. Zanchet, R. Landers and L. M. Rossi, *ACS Catal.*, 2012, **2**, 925–929; (*c*) T. O. Ely, C. Amiens, B. Chaudret, E. Snoeck, M. Verelst, M. Respaud and J. M. Broto, *Chem. Mater.*, 1999, **11**, 526–529.
23 O. Kysliak and A. Schnepf, *Dalton Trans.*, 2016, **45**, 2404–2408.
24 T. A. Albright, J. K. Burdett and M. H. Whangbo, *Orbital Interactions in Chemistry*, 2nd edn, 2013.
25 J. M. Goicoechea and S. Sevov, *Inorg. Chem.*, 2005, **44**, 2654–2658.